VIP ANR-09-COSI-03
Virtual Imaging Platform

M3.3.2 – Validation study of the brain model for MS USPIO-enhanced diagnosis

Fang Cao, Olivier Commowick, Elise Bannier, Alessandro Crimi, Christian Barillot

Abstract

This document describes our work towards establishing a relaxometry mapping of human brains. We provide an accurate estimation of T_1 relaxometry maps in order to use it as a quantifier of local inflammatory processes using USPIO contrast agent and apply this on multiple sclerosis. The framework will also be extended to T_2 and T_2^* relaxometry mapping, and then build the simulator for an object with pathological regions, with a realistic simulation of MRI contrast.

Contents

1 Introduction

This document is a preliminary report for the project "M3.3.2 – Validation study of the brain model for MS USPIO-enhanced diagnosis".

This project addresses one of the VIP major objectives: the modeling of inflammation process from MRI simulation. We intend to validate the simulation of molecular MR images in the context of neuro-inflamatory pathology. We will work in the context of ultra-small iron oxide nanoparticles (named USPIO) that are MRI contrast agents of high interest because they specifically mark macrophages.

In this project, we specifically work on the design of a virtual model to simulate MR images with different acquisition protocols. We will focus on an inflamed brain model as encountered in Multiple Sclerosis. The model will be used to simulate MR images of the neuro-inflammation process and validated from real MR relaxometry parameters as obtain on 3T MRI systems. The purpose of such simulated images is the modeling of MRI acquisition sequences in order to estimate high resolution quantitative imaging parameters able to exhibit the actual neuro-inflammation within Multiple Sclerosis lesions.

The main objective of this project is the construction of the input object for the MRI simulator. Each voxel of the object is defined by its physical properties, the 4 parameters T_1, T_2, T_2^* and M_0 (Fig. 1). In our case, this object represents a brain suffering from multiple sclerosis. Using these 4 physical parameters, we can simulate the weighted images of T_1-w, T_2-w, PD-w, FLAIR, etc., such as the sequences implemented in real measurement, whose acquisition parameters are known. In this project, we expect to establish a high-resolution mapping of T_1, T_2 and T_2^* in the areas of USPIO contrast enhancement, and in turn to build the simulator for an object with pathological regions.

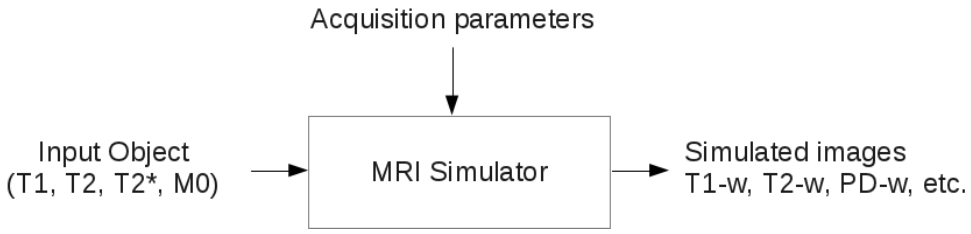

Figure 1: Construction of an input object for MRI simulator: T_1, T_2, T_2^* maps and M_0 image.

The first step is to generate the parameters T_1, T_2, T_2^* and M_0 of the input object. This can be modeled as an inverse problem with respect to relaxometry protocols. The unknowns to be determined are the parameters T_1, T_2, T_2^* and M_0 of the object, and the acquisition parameters and relaxometry sequences are known. In our case, the relaxometry sequences are defined in the specific acquisition protocol, USPIO–6. Each of the physical parameters T_1, T_2 and T_2^* is estimated independently. The idea is to estimate the physical parameters together with the equilibrium magnetization M_0 through a process of optimization with constraints. Let $(S_1, S_2, \ldots, S_n)$ the acquired relaxometry sequences with respect to the USPIO–6 protocol, and n equals to 2, 7 and 5 corresponding to distinct physical parameters T_1, T_2 and T_2^*. The flow diagram of the optimization process is presented in Fig. 2. The parameter sets (T_1, M_0), (T_2, M_0) and (T_2^*, M_0) are the estimations from these relaxometry sequences and acquisition parameters that depend on the MR imaging protocol.

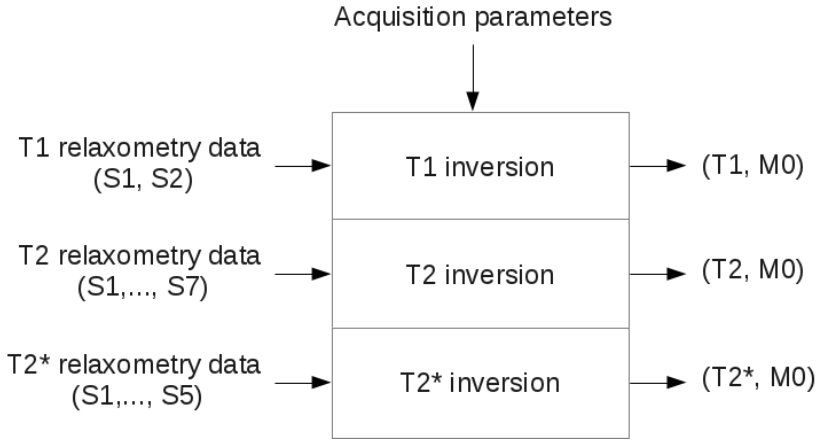

Figure 2: Estimation of physical parameters: T_1, T_2, T_2^* maps and M_0 image.

The maps T_1, T_2 and the image M_0 thus calculated will allow us to realistically simulate the MRI sequences (by construction, close to the actual MR images). In a second step, we will validate the maps T_1, T_2, T_2^* and M_0 (work in progress). It would be desirable that these maps do not conflict with the literature data or with data obtained in the relaxometry protocol.

In this report, we present our work on the T_1 and M_0 estimation, using the relaxometry data acquired in USPIO–6 protocol (Section 2 & 3). We propose an improved algorithm for the *DESPOT1* method. We also define a simplified model for simulation of Spin Echo sequence based on the Bloch equation (Section 4).

2 Methods

2.1 Background

We propose a new method to improve the T_1 mapping with respect to the popular *DESPOT1* algorithm. A constrained distance function is defined to model the distance between the pure signal and the measurements in presence of noise. We use a gradient descent optimization algorithm to iteratively find the optimal values of T_1 and M_0. The method is applied to MR images acquired with 2 gradient echo sequences and different flip angles. The performance of T_1 mapping is evaluated both on phantom and on in vivo experiments. Initial experiments are performed on acquisitions before and 24 hours after injection of USPIO in order to exhibit T_1 modifications related to the presence of macrophages in multiple sclerosis (MS) lesions.

The longitudinal relaxation time, T_1, is tissue specific at a given field strength. It can be measured to identify and differentiate healthy or pathological tissues, and is particularly relevant for clinical studies involving quantitative MRI analysis. Hence, T_1 relaxometry is now progressively used in neurological studies to investigate the structural modifications occurring during brain development [15].

Conventionally, T_1 maps can be estimated using saturation-recovery (SR) sequences with multiple repetition times or on inversion recovery (IR) sequences with multiple inversion times. However, these conventional sequences require long acquisition times in order to measure the longitudinal magnetization at multiple time points. Moreover, long

repetition times are needed for accurate T_1 measurements.

Several methods have been proposed to bring forth rapid and accurate T_1 relaxometry. The acquisition of high-resolution T_1 maps in a clinically acceptable time frame has been demonstrated with several approaches [6, 16, 18]. Currently, the most popular rapid and high-resolution T_1 estimation algorithm is Driven Equilibrium Single Pulse Observation of T_1 (*DESPOT1*) [11, 1], originally introduced in [4] and further investigated by [17, 7, 8]. Deoni *et. al.* [7] first extracted the T_1 map from a pair of gradient echo images with optimal flip angles, and showed that, using *DESPOT1*, a 3D acquisition of $1 \times 1 \times 1\text{mm}^3$ can be achieved in less than 8 minutes on a 1.5T scanner.

In practice, however, T_1 map estimation can be biased:

1. The explicit solution of T_1 is sensitive to noise, especially in the background and skull areas where the signal to noise ratio (SNR) is low.
2. Negative and extremely high T_1 values may appear in CSF and lesion areas due to the discontinuity and the locally high derivative of GRE equation.
3. Partial volume effects.
4. Acquisition artifacts.
5. Flip angle inaccuracy related to B_1 inhomogeneity.
6. T_1 changes related to temperature drift.

In this work, we focus on noise sensitivity and on the negative and extremely high values of T_1 (item 1 and 2), and improve T_1 mapping with respect to the popular *DESPOT1* algorithm. We propose a constrained distance function and use a gradient descent optimization algorithm to iteratively estimate the optimal T_1 value. Evaluation on phantom and on in vivo studies indicates the improvement of the T_1 measurement.

2.2 Basic *DESPOT1* Theory [3]

DESPOT1 uses a gradient echo sequence acquisition scheme [7]. The measured signal can be derived from the following equation:

$$S_\theta = \frac{M_0(1 - \exp(-TR/T_1))\sin\theta}{(1 - \exp(-TR/T_1)\cos\theta)} \tag{1}$$

θ: flip angle (MR acquisition parameter)

TR: repetition time (MR acquisition parameter)

S_θ: gradient-echo sequence with flip angle θ (the acquired image)

T_1: longitudinal relaxation time (unknown parameter, tissue specific at a given magnetic field strength)

M_0: equilibrium magnetization (unknown parameter, related to tissue and MR setup)

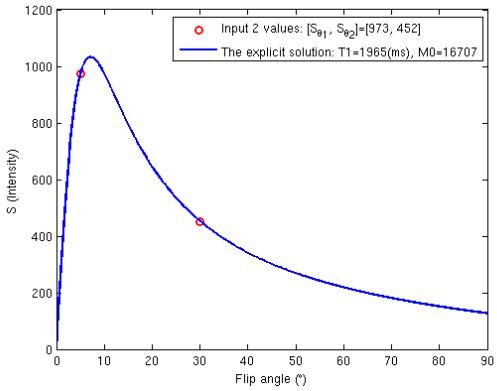

Figure 3: The simulated plot of signal S from 2 acquisitions $(S_{\theta 1}, S_{\theta 2})$ with flip angles θ_1 and θ_2: $\theta_1 = 5°$, $\theta_2 = 30°$, TR = 15ms, acquired on a human brain.

S_θ can be corrupted by noise, and θ can be inaccurate due to the acquisition related limitations. As demonstrated in [17], holding TR constant and changing θ, equation (1) can be reformulated as a simple linear equation

$$Y = aX + b \tag{2}$$

in which X and Y are parameterized as $Y = S_\theta / \sin\theta$ and $X = S_\theta / \tan\theta$. The slope and intercept are

$$a = \exp(-TR/T_1), b = M_0(1 - \exp(-TR/T_1)) \tag{3}$$

Thus, we can extract T_1 and M_0 from a and b

$$T_1 = -\frac{TR}{\ln b}, M_0 = \frac{a}{1-b} \tag{4}$$

From equation (2), we can find the explicit solution for T_1 and M_0 if we have 2 input signals ($S_{\theta 1}$ and $S_{\theta 2}$). Fig. 3 shows that acquiring 2 points $S_{\theta 1}$ and $S_{\theta 2}$, we can calculate the explicit solution of T_1 and M_0, and generate a solid curve with incrementally increasing θ. It should be noted that the factor M_0 only changes the absolute value of the signal intensity S_θ, not the shape of the curve.

2.3 *Optimized DESPOT1* Method

The basic *DESPOT1* algorithm provides an analytic solution for T_1 estimation. However, in the presence of noise, the analytic solution may not be the optimal value. For example, a background voxel (highly corrupted by noise) in a real brain image can get $S_{\theta 1}$ and $S_{\theta 2}$ equal to $S_{5°} = 7$ and $S_{30°} = 3$, leading to a T_1 value of 2245ms using *DESPOT1*. However, a calculated T_1 on a real gray matter voxel in the same image equals to 2493ms with $S_{5°} = 739$ and $S_{30°} = 298$. In this case, the T_1 values from the noise and from the signal are very close.

An intuitive method to suppress the influence of noise is to set thresholds to remove the background and skull signal before applying *DESPOT1*, and restrict T_1 estimation to a certain range [2]. However, choosing specific thresholds precludes the use of the method for multicenter studies, involving multiple MRI systems from different manufacturers with different image contrast and signal to noise ratio.

In this work, we have introduced an optimization algorithm to estimate the T_1 value without any prior knowledge on the images. We assume that, in the presence of noise, there are optimal values for the parameters $(\hat{T}_1, \hat{M}_0, \hat{\theta}_1, \hat{\theta}_2)$ with respect to an appropriate distance function. A gradient descent optimization algorithm is used to find the minimum of this cost function. The constrained distance function is defined as:

$$\underset{(\hat{\theta},\hat{T}_1,\hat{M}_0)}{\operatorname{argmin}} \left[\lambda|\hat{\theta} - \theta|^2 + (1-\lambda)|\mathbf{S}_{\hat{\theta}} - \mathbf{S}_{\theta}|^2\right] \tag{5}$$

$$\text{with} \quad \hat{\theta} = [\hat{\theta}_1, \hat{\theta}_2], \quad \theta = [\theta_1, \theta_2], \quad \mathbf{S}_{\hat{\theta}} = [S_{\hat{\theta}1}, S_{\hat{\theta}2}], \quad \mathbf{S}_{\theta} = [S_{\theta 1}, S_{\theta 2}]$$

- $S_{\theta 1}$ and $S_{\theta 2}$ are the acquired MR images
- θ_1 and θ_2 are the prescribed flip angles
- $\hat{\theta}_1$ and $\hat{\theta}_2$ are the estimated flip angles
- $\hat{T}_1$ and $\hat{M}_0$ are the estimated T_1 and M_0
- $\hat{\theta}$, $\hat{T}_1$, $\hat{M}_0$ and $S_{\hat{\theta}}$ follow the GRE equation
- λ is a constant scale factor to balance the 2 terms in the distance function
- We constrain $\hat{T}_1$ in the range of [1, 5000] based on prior knowledge on human body at 3T [10, 5, 14].

The algorithm starts from the initial values of $(\hat{T}_1 = 1, \hat{M}_0 = 0, \hat{\theta}_1 = \theta_1, \hat{\theta}_2 = \theta_2)$, and iteratively finds the first minimum. We allow the optimization to vary around nominal values of θ_1 and θ_2 because of the uncertainties on these parameters (modeled as noise here). We also found that it is necessary to include the estimation of $\hat{\theta}_1$ and $\hat{\theta}_2$ in the distance function in order to get the optimal value of T_1.

3 Results

We tested our algorithm on in vivo MR acquisitions performed on a 3T Siemens Verio (VB17) scanner with a 32-ch head coil. T_1 relaxation was calculated based on two gradient echo sequences acquired with flip angles of 5° and 30° as well as a repetition time of 15ms [9]. The voxel size was $1.3 \times 1.3 \times 3.0\text{mm}^3$.

3.1 Synthetic Experimental Results on Sample Points

We found that our proposed algorithm is efficient to correct 3 typical types of errors in T_1 mapping.

Error 1: $T_1 \leq 0$ which is not possible (Fig. 4(a)). This error usually occurs in lesion and CSF areas. Since we are interested in the further study of these lesions, such errors should be removed before the quantitative analysis.

Error 2: Extremely high T_1 values, e.g. above 20000ms in CSF, which are not expected (Fig. 4(c)).

Error 3: $S_{\theta 1}$ and $S_{\theta 2}$ are pure noise, and the estimated T_1 value should be close to 0 (Fig. 4(e)). This error usually occurs in background and the air filled cavities in the skull.

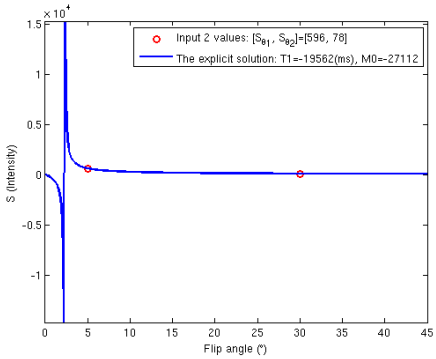

(a) Error 1: $T_1 \leq 0$

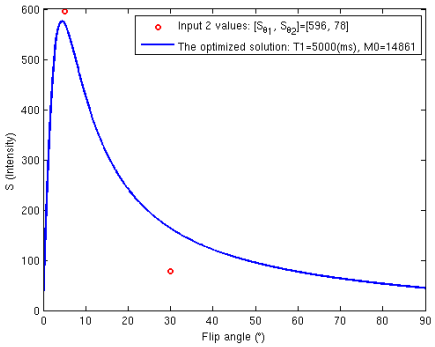

(b) Optimized results for error 1

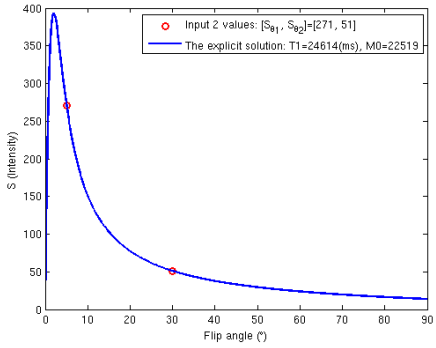

(c) Error 2: Extremely high T_1

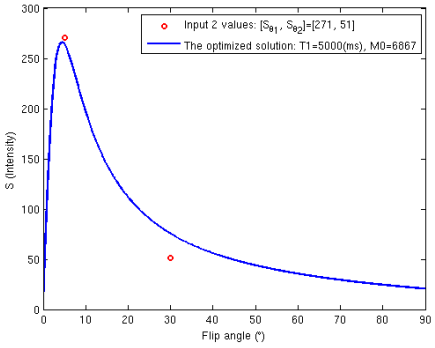

(d) Optimized results for error 2

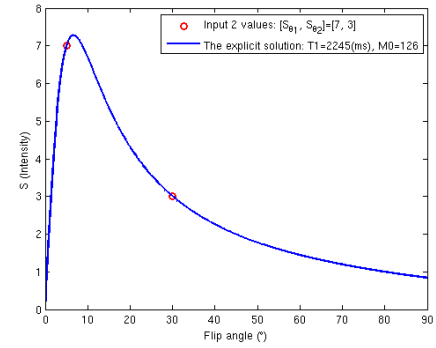

(e) Error 3: Voxels with low SNR

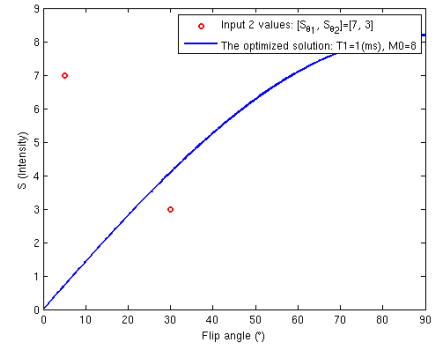

(f) Optimized results for error 3

Figure 4: Left column gives 3 different kinds of errors in the basic *DESPOT1* method. Right column gives the corresponding results of *optimized DESPOT1* algorithm. The ($S_{\theta 1}$, $S_{\theta 2}$) pairs are chosen from in vivo brain measurements.

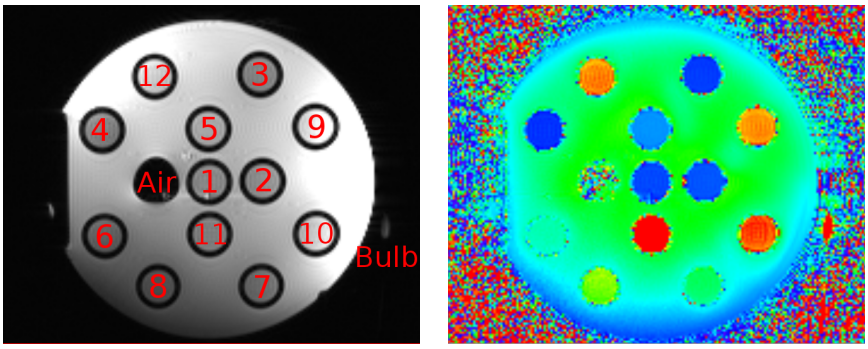

(a) The input $S_{\theta 1}$ (b) Basic *DESPOT1*

(c) *DESPOT1 with thresholds* [2] (d) *Optimized DESPOT1*

Figure 5: Comparison of the T_1 maps from the basic *DESPOT1*, *DESPOT1 with thresholds* and *optimized DESPOT1* on the TO4 SpinSafety phantom.

Fig. 4(b,d,f) shows the improvement over the basic *DESPOT1* algorithm for these 3 types of errors. The sample points are chosen from in vivo brain measurements.

3.2 Phantom Experimental Results

We performed phantom experiments to quantitatively evaluate the results of T_1 estimation. The TO4 phantom of the SpinSafety test-objects[1] is made especially for T_1 accuracy assessment [13]. It contains 12 tubes filled with solutions having known T_1 relaxation times. The tube numbers are shown in Fig. 5(a). Tubes 1, 6, 9, 10 and 11 have T_1 values similar to the human brain (see reference T_1 values in Tab. 1). It should be noted that the reference T_1 values have a variance of 20%.

We compared the T_1 maps with the basic *DESPOT1*, *DESPOT1 with thresholds* and our algorithm (Fig. 5). The empty tube (Air) is not visible in Fig. 5(b) with basic *DESPOT1*, but we can see it clearly in Fig. 5(d) with the proposed method. Tube 6, 7 and 8 can be clearly identified in Fig. 5(d). There is also a bulb of the thermometer which was used to monitor the temperature during the acquisition. The bulb is clearly identified in the T_1 map of *optimized DESPOT1* showing that the proposed method can be used for target identification. *Optimized DESPOT1* yields improved results as compared to the basic *DESPOT1* and *DESPOT1 with thresholds*. We also found that even there

[1]The SpinSafety® test-objects (Spin Safety Ltd, Rennes, France) is a commercially available version of the Eurospin test-objects.

Tube	R(ms)	Estimating T_1 (ms)		RD (%)
		μ	δ	
1	107	94.6334	6.6591	11.5576
2	115	102.8524	3.4007	10.5631
3	98	86.4381	3.4564	11.7979
4	91	80.0732	3.6266	12.0075
5	162	143.2431	3.2002	11.5783
6	301	258.3710	6.6461	14.1624
7	360	309.7457	10.3142	13.9595
8	518	447.2865	18.0648	13.6513
9	703	599.4820	14.3356	14.7252
10	770	652.4993	24.4054	15.2598
11	1092	951.1581	40.9323	12.8976
12	719	607.3630	21.9891	15.5267

Table 1: Quantitative analysis of the precision of T_1 map for the proposed method: R is the reference T_1 value (20% variance), μ the estimated mean value and δ the standard deviation for Gaussian modeling. RD is the relative deviation defined by $|\mu - R|/R$ (%).

is an obvious intensity bias in $S_{\theta 1}$ and $S_{\theta 2}$ (see the intensity variation in Fig. 5(a)), the estimated T_1 map is not very sensitive to the bias effect.

We found that the histogram of the T_1 values in each tube can be modeled as a Gaussian distribution. We utilize an iterative least squares method to estimate the mean value μ and standard deviation σ from the histogram of each tube. We found that the results from different algorithms are without significant difference inside each tube. The estimated μ and σ for the *optimized DESPOT1* method, together with the reference T_1, are given in Tab. 1. The relative deviation (RD) is between 10% and 16% in all the cases. This represents that the estimated μ falls well in the range of the reference value, considering the accuracy of the reference T_1 value is 20%. The standard deviation is small (< 20) in most cases, except from tubes with high reference T_1 values (tube 10,11,12). Considering tube 11 with the highest reference T_1 value (1092ms), the corresponding standard deviation is over 40. This shows that the variation is increasing as the T_1 value increases.

3.3 Brain T_1 Mapping

We compared our algorithm with the basic *DESPOT1* and *DESPOT1 with thresholds* on multiple sclerosis (MS) patients. The results of the basic *DESPOT1* are very sensitive to noise. *DESPOT1 with thresholds* shows improved results but the thresholds need to be chosen carefully not to preclude T_1 estimation in tissue regions with low SNR, such as the vessels in the lower part of the brain (Fig. 8(b)). Our proposed method is well adapted to suppress noise in the air. It is also effective to preserve the tissue signal with low SNR in noisy regions, and it removes the discontinuity effect of black holes in lesions and CSF.

Optimized DESPOT1 algorithm improves the brain T_1 mapping in 3 aspects.

1. Remove the black holes in lesions (Fig. 6).

2. Improve the identification of arteries which are surrounded by CSF in the lower part of the brain (Fig. 7).

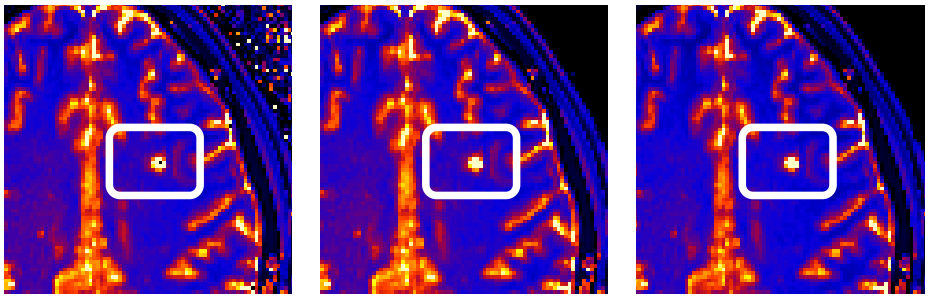

(a) Basic *DESPOT1* (b) *DESPOT1 with thresholds* (c) *Optimized DESPOT1*

Figure 6: Comparison of the T_1 maps with different methods: **Lesion area**

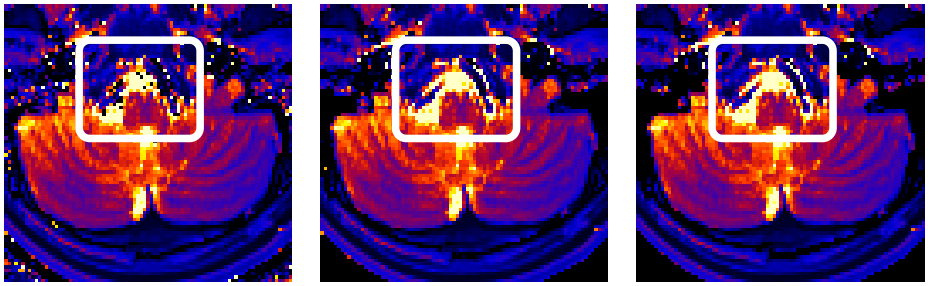

(a) Basic *DESPOT1* (b) *DESPOT1 with thresholds* (c) *Optimized DESPOT1*

Figure 7: Comparison of the T_1 maps with different methods: **CSF area**

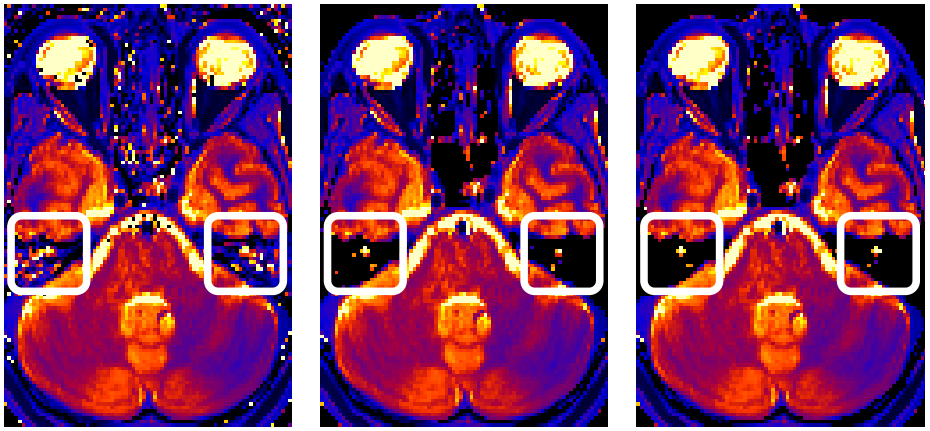

(a) Basic *DESPOT1* (b) *DESPOT1 with thresholds* (c) *Optimized DESPOT1*

Figure 8: Comparison of the T_1 maps with different methods: **Low SNR area**

DESPOT1 with thresholds and *optimized DESPOT1* remove the discontinuity effect of black holes in lesions and CSF (near arteries). *Optimized DESPOT1* shows the best performance to suppress noise in the lower part of the brain and preserve the tissue signal with low SNR.

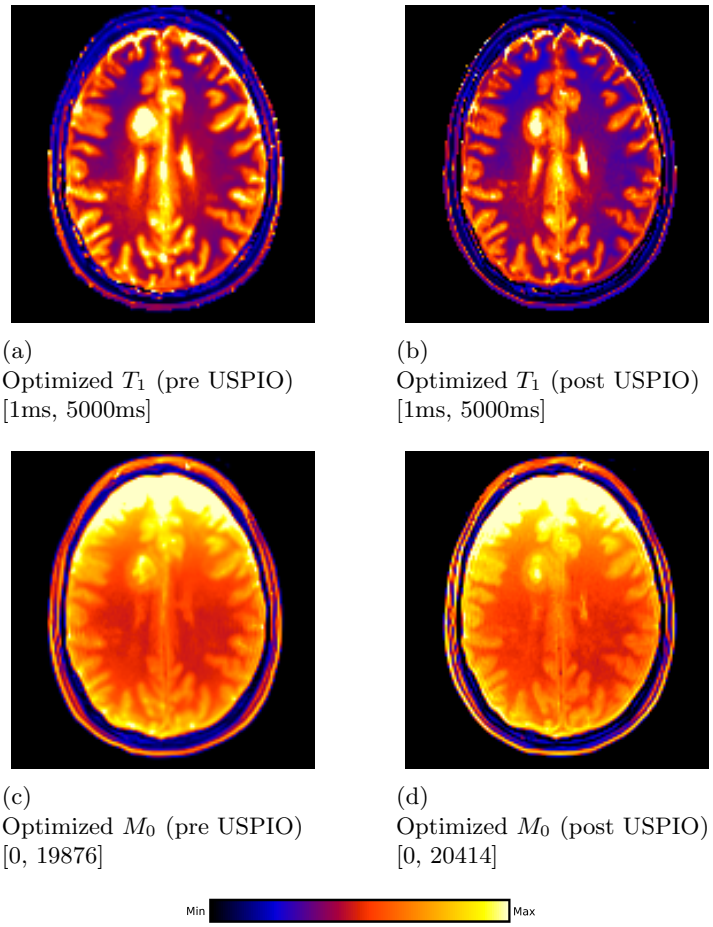

(a)
Optimized T_1 (pre USPIO)
[1ms, 5000ms]

(b)
Optimized T_1 (post USPIO)
[1ms, 5000ms]

(c)
Optimized M_0 (pre USPIO)
[0, 19876]

(d)
Optimized M_0 (post USPIO)
[0, 20414]

Figure 9: T_1 maps and M_0 images before and after the injection of USPIO. [min, max] gives the range of the colorbar for each image.

3. Suppress noise in low SNR areas, for example the air filled cavities in the skull (Fig. 8).

3.4 Results on MS Patients (USPIO)

The proposed method was applied to multiple sclerosis (MS) patients who underwent on experimental study where the T_1 relaxometry data were recorded before and after the injection of USPIO contrast agent. This is a previous work to exhibit T_1 modifications related to the presence of macrophages and local inflammatory processes in MS lesions.

An example of the estimated difference of T_1 map according to the proposed method is shown in Fig. 9. We found clear difference in the T_1 map before and after the injection of USPIO. The M_0 images calculated by our algorithm are also given in Fig. 9. On the M_0 image, the contrast between CSF and white matter is coherent with the variation of proton density in different tissues. It can be noted that the M_0 image is more sensitive to the inhomogeneity bias in the native images than the quantitative T_1 map.

We give the T_1 maps before and after USPIO injection, as well as the difference (Fig. 10). The lesion areas are clearly enhanced by the presence of USPIO in the contrast images.

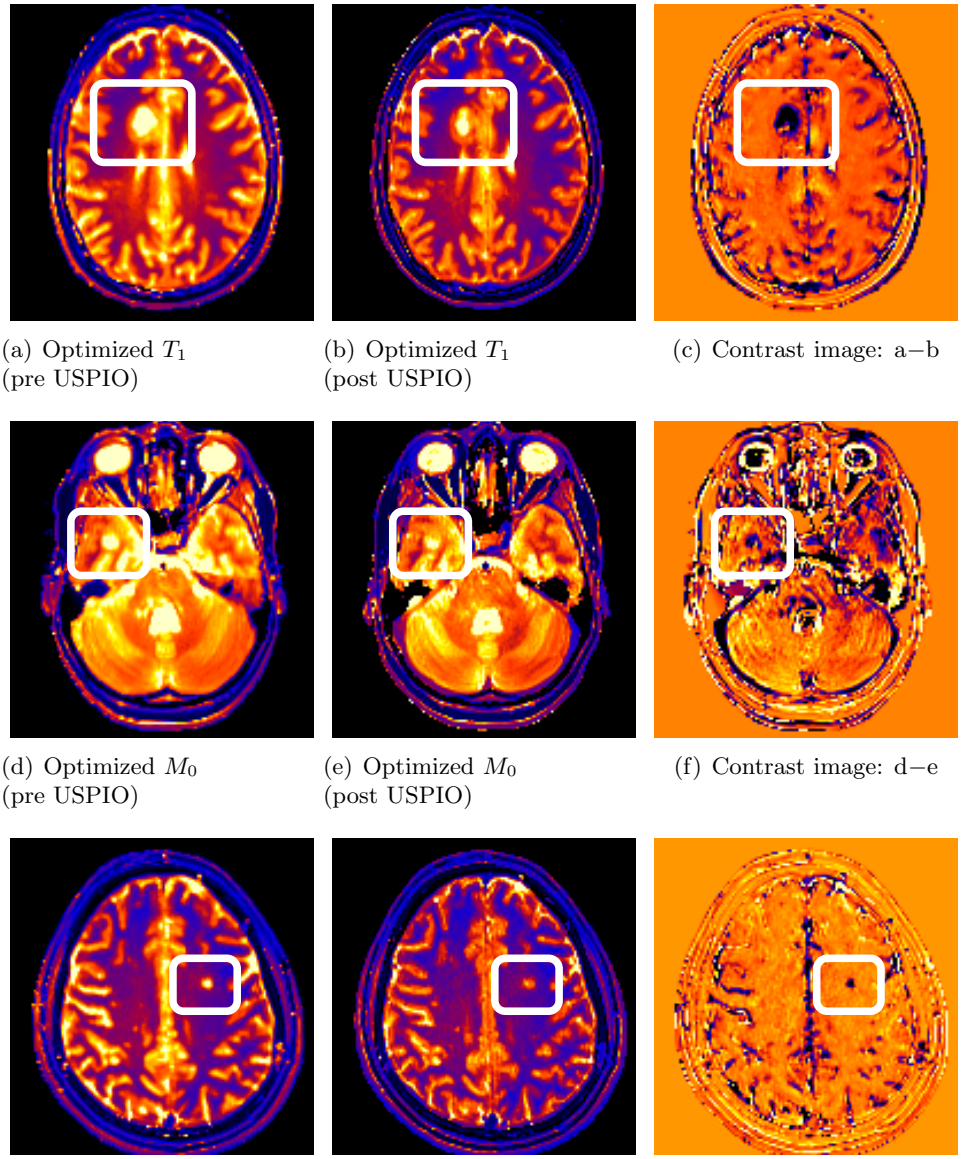

(a) Optimized T_1 (pre USPIO)
(b) Optimized T_1 (post USPIO)
(c) Contrast image: a−b
(d) Optimized M_0 (pre USPIO)
(e) Optimized M_0 (post USPIO)
(f) Contrast image: d−e
(g) Optimized M_0 (pre USPIO)
(h) Optimized M_0 (post USPIO)
(i) Contrast image: g−h

Figure 10: T_1 maps pre/post USPIO and the difference in lesions.

4 Simulator: *SimuBloch* v0.1

The simulator *SimuBloch* is made for a fast simulation of signal sequences based on Bloch equation. It can be run directly from the VIP Portal: http://vip.creatis.insa-lyon.fr. The current version is v0.1, which allows to simulate a Spin Echo sequence using the following function:

$$S = M_0(1 - \exp(-TR/T_1))\exp(-TE/T_2) \tag{6}$$

The simulator is given in Fig. 11.

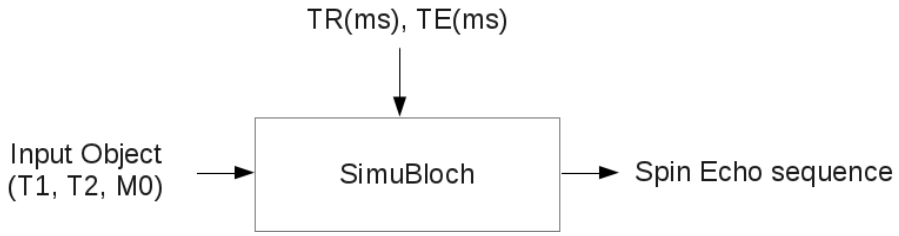

Figure 11: Construction of the Spin Echo sequence with the simulator *SimuBloch*.

- Input image files (Mandatory)
  - T_1: Longitudinal (or spin-lattice) relaxation time (ms).
  - T_2: Transverse (or spin-spin) relaxation time (ms).
  - M_0: Equilibrium magnetization, which is proportional to proton density ρ.

  The dimensions and sizes of the input images should be equal.

- Input parameters
  - TR: Repetition time (ms). The value should be ≥ 0. The default value is 500ms.
  - TE: Echo time (ms). The value should be ≥ 0. The default value is 8.4ms.

  TR and TE should follow the condition $TE < TR$. If the parameters are not set by the user, the simulator uses the default values to compute the sequence.

- Output image file (Mandatory)
  - S: Spin Echo sequence.

The image formats are those supported by the ITK library[2]. The dimension can be 1D, 2D or 3D. The simulator was tested with 3D images in the nifti format.

From a 3D virtual object with parameters T_1, T_2 and M_0, we can compute the Spin Echo sequence using the simulator for 3 basic MRI scans (choice of TR and TE for conventional Spin Echo sequences is taken from [12]).

- T_1-weighted: Short TR (less than 750ms), short TE (less than 40ms).
  An example for T_1-w simulation is given in the package *SimuBloch* with $TR = 500ms$ and $TE = 8.4ms$.

[2] http://www.itk.org/

- T_2-weighted: Long TR (more than 1500ms), long TE (more than 75ms).
  An example for T_2-w simulation is given in the package *SimuBloch* with $TR = 6530ms$ and $TE = 84ms$.
- PD-weighted: Long TR (more than 1500ms), short TE (less than 40ms).
  An example for PD-w simulation is given in the package *SimuBloch* with $TR = 6530ms$ and $TE = 9.4ms$.
- The sample data can be found in the package *SimuBloch* v0.1.

One example of the simulated T_1-weighted image is given in Fig. 12. We found a good consistency with the image obtained in real measurement.

5 Conclusion

We propose a new analytic MRI simulator for Spin Echo MR images which takes as argument real or synthetic T_1, T_1 and ρ (M_0) maps. In order to estimate these maps, we have developed a new estimation algorithm that uses standard relaxometry images and finds an optimal solution to improve the SNR of the estimated T_1 map and M_0 image. This new estimator is performed by optimizing a new distance function to generate the optimal values of T_1 and M_0 in presence of noise. A gradient descent optimization algorithm is provided to give reliable T_1 estimation. This estimator has been validated on a phantom through real MRI acquisition, and the resulting images have been made available for use with the analytic MRI simulator on the VIP platform. Further work will focus on extending the algorithm and assessing the method on a large database of MS patients. The framework will also be extended to T_2 and T_2^* relaxometry mapping. This will in turn build the simulator for an object with pathological regions, with a realistic simulation of MRI contrast.

References

[1] Hasan Bagher-Ebadian, Rajan Jain, Ramesh Paudyal, Siamak P. Nejad-Davarani, Jayant Narang, Quan Jiang, Tom Mikkelsen, and James R. Ewing. Magnetic resonance estimation of longitudinal relaxation time (T1) in spoiled gradient echo using an adaptive neural network. In *IJCNN*, pages 2557–2562, 2011.

[2] Fang Cao, Olivier Commowick, Elise Bannier, Jean christophe Ferre, Gilles Edan, and Christian Barillot. T1 and T2 mapping in patients with multiple sclerosis for project USPIO–6. In *ARSEP 2012*, Jun 2012.

[3] Fang Cao, Olivier Commowick, Elise Bannier, Jean christophe Ferre, Gilles Edan, and Christian Barillot. MRI estimation of t_1 relaxation time using a constrained optimization algorithm. In *MBIA 2012*, 2012, submitted.

[4] Kenner A. Christensen, David M. Grant, Edward M. Schulman, and Cheves Walling. Optimal determination of relaxation times of fourier transform nuclear magnetic resonance. determination of spin-lattice relaxation times in chemically polarized species. *J Phys Chem*, 78(19):1971–1977, 1974.

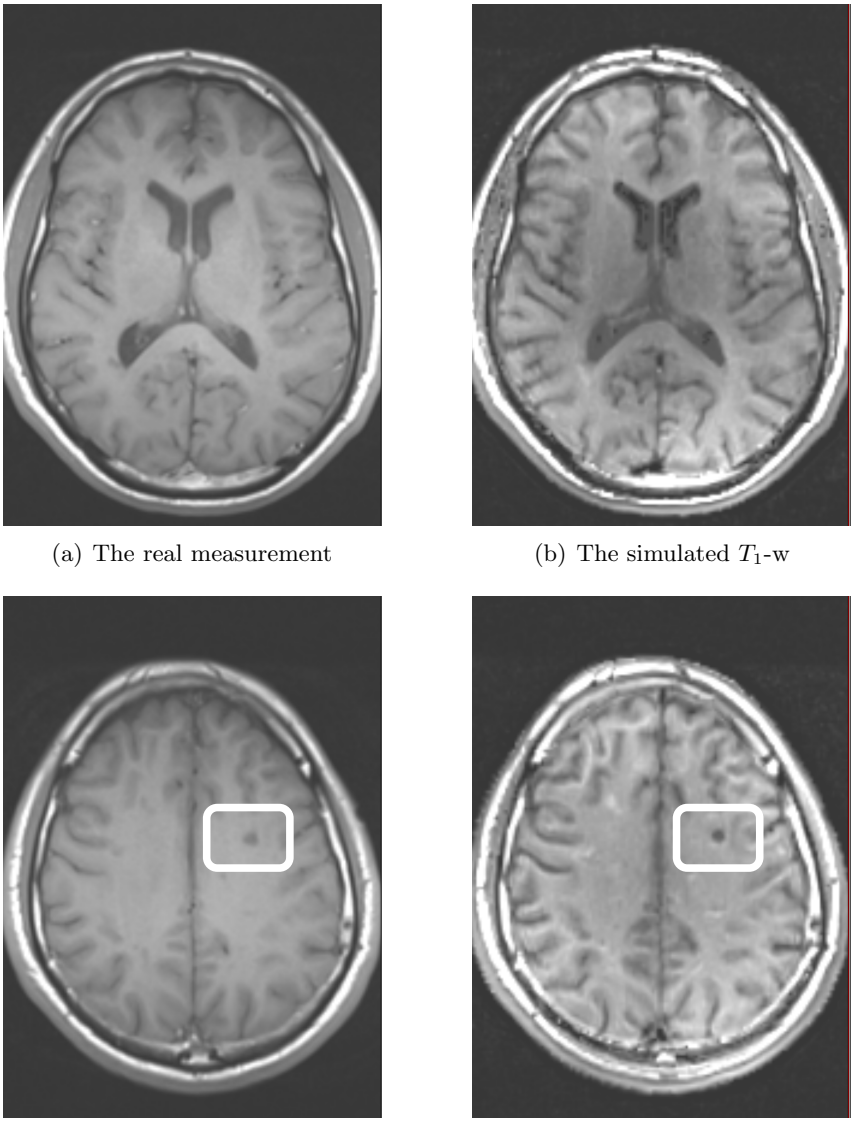

(a) The real measurement

(b) The simulated T_1-w

(c) The real measurement (MS lesion)

(d) The simulated T_1-w(MS lesion)

Figure 12: The simulated T_1-weighted image and the real measurement. The results are registered to the same template and present in the same gray level.

[5] Charuta Dagia and Michael Ditchfield. 3t mri in paediatrics: challenges and clinical applications. *Eur J Radiol*, 68(2):309–319, 2008.

[6] R Deichmann, D Hahn, and A Haase. Fast T1 mapping on a whole-body scanner. *MRM*, 42(1):206–209, 1999.

[7] S.C. Deoni, B.K. Rutt, and T.M. Peters. Rapid combined T1 and T2 mapping using gradient recalled acquisition in the steady state. *MRM*, 49(3):515–526, 2003.

[8] Sean C L Deoni, Terry M Peters, and Brian K Rutt. Determination of optimal angles for variable nutation proton magnetic spin-lattice, T1, and spin-spin, T2, relaxation times measurement. *MRM*, 51(1):194–199, 2004.

[9] J.-C. Ferré, A. Tourbah, I. Berry, C. Barillot, L. Freeman, D. Galanaud, A. Maarouf, J. Pelletier, C. Portefaix, J. P. Ranjeva, N. Wiest-Daesslé, and G. Edan. MRI USPIO analysis in 35 clinically isolated syndrome patients. In *ECTRIMS'2011*, number 5, pages 399–416, Nov 2011.

[10] N. Gelman, J.M. Gorell, P.B Barker, R.M Savage, E.M. Spickler, J.P. Windham, and R.A. Knight. MR imaging of human brain at 3.0T: preliminary report on transverse relaxation rates and relation to estimated iron content. *Radiology*, 210(3):759–767, 1999.

[11] C Lee, E Baker, and D Thomasson. *Normal Regional T1 and T2 Relaxation Times of the Brain at 3T*, page 959. 2006.

[12] D.W. McRobbie. *MRI from Picture to Proton*. Cambridge University Press, 2003.

[13] S. Ollivro, P. Eliat, E. Hitti, L. Tran, J.D. de Certaines, and H. Saint-Jalmes. Preliminary MRI quality assessment and device acceptance guidelines for a multicenter bioclinical study: The GO glioblastoma project. *J Neuroimaging*, 2011.

[14] G.J. Stanisz, E.E Odrobina, J. Pun, M. Escaravage, S.J. Graham, M.J. Bronskill, and R.M. Henkelman. T1, T2 relaxation and magnetization transfer in tissue at 3T. *MRM*, 54(3):507–512, 2005.

[15] P. Tofts. *Quantitative MRI of the Brain: Measuring Changes Caused by Disease*. John Wiley & Sons, Ltd, 2003.

[16] Lalitha Vaithianathar, Chris R Tench, Paul S Morgan, and Cris S Constantinescu. Magnetic resonance imaging of the cervical spinal cord in multiple sclerosis–a quantitative T1 relaxation time mapping approach. *J Neurology*, 250(3):307–315, 2003.

[17] H. Z. Wang, S. J. Riederer, and J. N. Lee. Optimizing the precision in T1 relaxation estimation using limited flip angles. *MRM*, 5(5):399–416, Nov 1987.

[18] Jinghua Wang, Maolin Qiu, Hyeonjin Kim, and R Todd Constable. T1 measurements incorporating flip angle calibration and correction in vivo. *J Magn Reson*, 182(2):283–292, 2006.